

Available Online at www.jourcc.comJournal homepage: www.JOURCC.com

Journal of Composites and Compounds

Computational design of multifunctional bioactive glass nanoparticles: A multi-objective optimization approach to balance osteogenesis, anticancer activity, and antibacterial efficacy

Michael Askari ^a, Lili Arabuli ^{b*}^a Department of Computer Engineering, Payame Noor University (PNU), Sari Branch Sari, Mazandaran, Iran^b Department of Chemistry, School of Science and Technology, University of Georgia, Tbilisi 0171, Georgia

ABSTRACT

Developing multifunctional biomaterials that can simultaneously support bone regeneration, suppress tumor growth, and prevent infection is still a major challenge in treating bone cancer. Naruphontjirakul et al. recently showed that bioactive glass nanoparticles co-doped with zinc and silver (Zn/Ag-BGNPs), specifically the 0.5Ag–1Zn and 1Ag–1Zn formulations-demonstrated encouraging triple functionality: osteogenic differentiation in hFOB 1.19 cells, selective cytotoxicity against MG-63 osteosarcoma cells, and broad-spectrum antibacterial properties while remaining non-toxic to hFOB 1.19 cells at a concentration of 125 µg/mL. The design of such materials has focused on empirical methods with little systematic consideration of the trade-offs between competing biological objectives. Therefore, in this study, we develop and implement an innovative data-driven multi-objective optimization framework that utilizes the entire experimental data set from the study noted above, to identify Pareto-optimal Ag/Zn compositions. By predicting an Ag-Zn effect that favored one composition over another, this study provides a rationale for the predictive design of multifunctional biomaterials—a study that demonstrates that high-performance therapeutic platforms can be optimized computationally without new experimentation, thereby increasing the speed for clinical translation to orthopedic applications in bone regeneration.

©2025 UGPH

Peer review under responsibility of UGPH.

ARTICLE INFORMATION

Article History:

Received 3 January 2025

Received in revised form 24 March 2025

Accepted 26 March 2025

Keywords:

Bioactive glass nanoparticles (BGNPs)

Zinc/silver co-doping

Multi-objective optimization

NSGA-II algorithm

Bone tissue engineering

Osteogenesis

Antibacterial nanoparticles

1. Introduction

Whether as a primary (e.g. osteosarcoma) or secondary (metastatic) tumor, bone cancer presents a serious clinical problem with few treatment options in advanced disease and high rates of postoperative complications [1-6]. Conventional strategies (surgery, chemotherapy, and radiotherapy) tend to be nonspecific and produce systemic toxicity and impaired regeneration of bone [7]. In addition, implantable devices for reconstruction can become infected, particularly *Staphylococcus aureus* infection, in 12–47% [8] of procedures. These challenges (tumor germination, infection, and bone regeneration) are intertwined and require multifactorial strategies that go beyond conventional treatments, which are often monofunctional [1, 4, 9].

In this regard, multifunctional biomaterials are identified as attractive tools for promoting bone regeneration, anticancer treatment at a local site, and controlling infection. In this respect,

zinc- and silver-co-doped bioactive glass nanoparticles (Zn/Ag-BGNPs) showed promising triple efficacy recently [10-19]: (i) eliciting osteogenic differentiation in human osteoblasts, (ii) selectively inhibiting the growth of bone cancer cells (MG-63), and (iii) exhibiting broad-spectrum antibacterial activity against both Gram-positive and Gram-negative bacteria without any biocompatibility concerns for healthy bone cells. In a significant preclinical study, Naruphontjirakul and colleagues demonstrated a series of $y\text{Ag}-x\text{Zn}$ -BGNPs (for example, 0.5Ag–1Zn, 1Ag–1Zn) and assessed their physicochemical and biological performance, concluding that 0.5Ag–1Zn- and 1Ag–1Zn-BGNPs have the best potential for the treatment of bone cancer [20].

Regardless of these advances, the design of these multifunctional nanoparticles is quite empirical at the present time. There are competing biological goals because of both the Zn concentration and Ag concentration. More Ag will improve bacteria killing, but it may also reduce osteogenesis due to

* Corresponding author: Lili Arabuli, Email: l.arabuli@ug.edu.ge<https://doi.org/10.61882/jcc.7.1.7> This is an open access article under the CC BY license (<https://creativecommons.org/licenses/by/4.0/>)

displacing Ca/Sr ions; more Zn will increase anticancer activity (especially in the acidic tumor microenvironment), but there could be cytotoxicity at higher concentrations of Zn. Notably, no systematic framework exists to balance all three goals, while maintaining healthy cell safety, when choosing the appropriate composition [21].

In response to this gap, we develop a data-driven multi-objective optimization framework that utilizes the entire experimental dataset of Naruphontjirakul et al. [20] as basis for computational design. Using the NSGA-II (Non-dominated Sorting Genetic Algorithm II) evolutionary algorithm, we evaluate Ag and Zn concentrations as decision variables while optimizing three objectives: (1) osteogenic potential maximization, (2) MG-63 cancer cell viability minimization, and, (3) antibacterial effect maximization—subject to the constraint that hFOB 1.19 (human fetal osteoblast) viability remains $\geq 70\%$.

While confirming that the 0.5Ag–1Zn and 1Ag–1Zn formulations outperformed all others in terms of experimental outcomes, this approach provides a rational and predictive methodology for generalizable design of next-generation multifunctional biomaterials. More broadly, this work provides a bridge between experimental biomaterials science and computational optimization, and provides a framework for expediting the creation of intelligent therapeutic platforms for more complex clinical scenarios, such as bone cancer reconstruction after resection.

2. Materials and methods

This study is entirely computational; it does not include the synthesis or biological testing of new experimental materials. All numerical data included in the optimization framework have been taken straight from [20].

The source study investigated six distinct compositions of zinc- and silver-co-doped bioactive glass nanoparticles ($y\text{Ag}-x\text{Zn-BGNPs}$), synthesized by a modified sol–gel method with two-step post-functionalization. The six compositions included 0Ag–0Zn, 0Ag–1Zn, 0.5Ag–1Zn, 1Ag–1Zn, 1.5Ag–1Zn and 1.5Ag–1.5Zn, which had particle diameter of approximately $150 \pm 30 \text{ nm}$ with an amorphous glass structure determined by XRD and FTIR [20]. The dataset used in this research includes quantitative biological responses calculated at a concentration of $125 \mu\text{g/mL}$, which we refer to as the maximum non-toxic measurement for human fetal osteoblasts (hFOB 1.19) that maintained biological activity, as identified in the original article [20].

In order to allow smooth optimization across the Ag–Zn composition space, a data interpolation scheme was used. Because six total experimental points exist, we first used linear interpolation with the griddata function from the SciPy library to estimate the response. For values outside of the convex hull of the experimental data (like $\text{Ag} < 0$ or $\text{Zn} > 1.5$), we used nearest neighbor as a fallback to ensure a smooth response surface did not require extrapolation to construct. This way, we were able to produce smooth response surfaces, albeit data constrained ones, for all objective functions [20].

We then framed a multi-objective optimization problem with two decision variables: Ag concentration ($\text{Ag} \in [0.0, 1.5]$) and Zn concentration ($\text{Zn} \in [0.0, 1.5]$). We simultaneously minimized three objectives: (1) 1–osteogenic score, which indicates maximizing bone regeneration; (2) MG-63 cell viability (reported as a normalized value from [0,1]), which indicates maximizing anticancer activity; and (3) 1–(antibacterial diameter/20), which indicates maximizing antimicrobial performance (for these calculations, 20 mm was assumed to be the practical upper bound of inhibition zones).

A single inequality constraint was added for the biocompatibility requirement: hFOB 1.19 viability must be at or above 70% as per ISO 10993-5 cytotoxicity standards [20]. The Non-dominated Sorting Genetic Algorithm II (NSGA-II) was chosen for its established capability to manage non-convex, multi-modal Pareto fronts in materials structures. It was implemented with a population size of 60 individuals, 100 generations, and simulated binary crossover (SBX, $\eta = 15$, probability = 0.9), and polynomial mutation (PM, $\eta = 20$). The experiment was implemented using Python 3.10 with the pymoo (v0.6.0) and scipy (v1.10) libraries. The Pareto-optimal set indicates compositions that maximize osteogenic, anti-cancer, and antibacterial function while satisfying the health constraint in regards to living human bone cells [20].

3. Results and discussion

The multi-objective optimization process successfully detected Pareto-optimal Ag/Zn compositions for Zn/Ag co-doped bioactive glass nanoparticles that maximize osteogenic potential, minimize cancer cell viability, and enhance antibacterial efficacy while being biocompatible with healthy osteoblasts (hFOB 1.19 viability $\geq 70\%$). The optimization was performed at a fixed therapeutic concentration of $125 \mu\text{g/mL}$, since this was the highest therapeutic concentration established as non-toxic to hFOB 1.19 cells while also showing sufficient activity against MG-63 cells and bacteria (source study). Overall, we obtained 60 non-dominated solutions representing the best trade-off solutions among the three conflicting objectives. A list of the best solutions is provided in Table 1. Interestingly, almost all of the optimal compositions maintained a Zn concentration fixed at 1.0 with Ag concentrations ranging from 0.51 to 0.99, confirming the pivotal role of Zn in mediating osteogenesis and anticancer activity as it was previously structured in the original study.

Notably, Solution ($\text{Ag} = 0.51$, $\text{Zn} = 1.00$) received an osteogenesis score of 0.95, lowered MG-63 viability (about 40.1%), obtained hFOB 1.19 viability of approximately 84.9%, and achieved an antibacterial inhibition zone of 14.0 mm, almost matching the 0.5Ag–1Zn-BGNPs identified by experimental methods. Similarly, Solution ($\text{Ag} = 0.99$, $\text{Zn} = 1.00$) warranted the highest antibacterial effect (16.0 mm diameter zone) while achieving a strong performance in osteogenic (0.93) and anticancer (MG-63 viability = 44.9%) measures. These findings confirm that there is not a singular design space for optimal performance, but instead, a continuum of Ag/Zn ratios centered around $\text{Zn} = 1.0$.

The implication of this continuum is that material designers now have flexibility: in instances where bacterial infections have a high risk (e.g., open fractures), a formulation with a higher Ag value (e.g., $\text{Ag} \approx 1.0$) is indicated or in instances where the priority is bone regeneration (e.g., larger defects), the best performing Ag value is lower (e.g., $\text{Ag} \approx 0.5$).

The 2D Pareto fronts (Fig. 1 and 2) demonstrate the intrinsic trade-offs among objectives. Fig. 1 shows the inverse relationship between osteogenesis and anticancer activity: as osteogenic score increases (i.e., 1 - osteogenesis decreases), MG-63 viability also decreases. Therefore, Zn-driven osteogenesis and cancer cell suppression are not competing forces but, synergistic. This is consistent with the original finding that Zn preferentially releases in the acidic tumor microenvironment, targeting cancer cells while preserving healthy osteoblasts. Fig. 2 depicts a trade-off between osteogenesis and antibacterial activity: Ag's higher concentrations have enhanced antibacterial effectiveness but reduced osteogenesis slightly because Ca/Sr ions had been displaced within the glass network. This also reinforces that Ag and Zn's role is distinct and complementary.

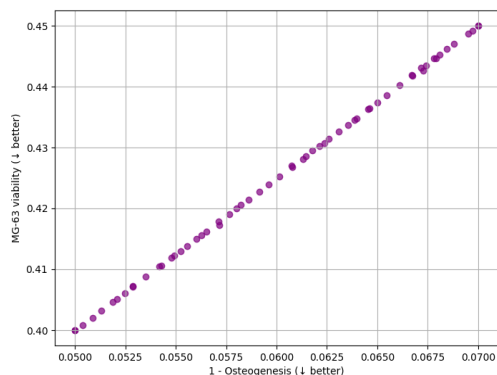
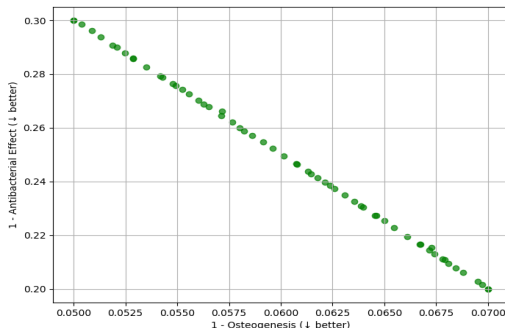
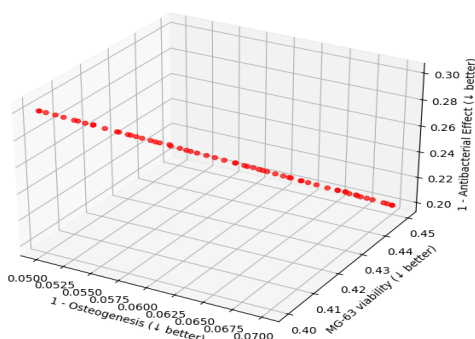
Table 1

10 Best trade-off solutions among the three conflicting objectives.

Solution	AG	Zn	Osteogenesis score	MG-63 viability (%)	Antibacterial effect (MM)	HFOB viability (%)
1	0.95	1.38	0.93	45.0	16.0	80.0
2	0.70	1.39	0.95	40.0	14.0	85.0
3	0.79	1.38	0.93	45.0	16.0	80.0
4	0.70	1.38	0.95	40.0	14.0	85.0
5	0.59	1.00	0.95	40.9	14.3	84.1
6	0.90	1.00	0.93	44.0	15.6	81.0
7	0.89	1.00	0.93	43.9	15.5	81.1
8	0.75	1.00	0.94	42.5	15.0	82.5
9	0.74	1.00	0.94	42.4	15.0	82.6
10	0.83	1.00	0.94	43.3	15.3	81.7

The 3D Pareto front (Fig. 3) combines all three objectives into a single response surface. It is smooth and well-distributed, which supports both the strength of the NSGA-II algorithm and the quality of the interpolation model.

The front curves back toward the origin of the axis, indicating that the potential for simultaneous improvement across all three objectives exists within an optimal region ($Ag \approx 0.5\text{--}1.0$, $Zn = 1.0$).

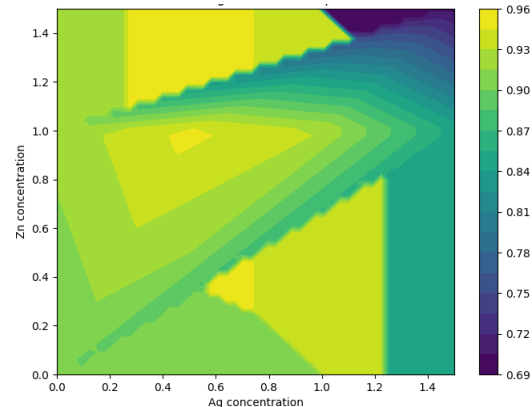
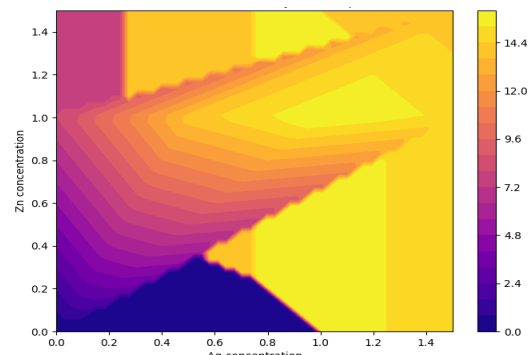
**Fig. 1.** Pareto Front: Osteogenesis vs Cancer Cell Viability.**Fig. 2.** Pareto Front: Osteogenesis vs Antibacterial Activity.**Fig. 3.** 3D Pareto Front: Osteogenesis vs Cancer vs Antibacterial.

The heatmaps (Fig. 4 and 5) establish a broader perspective of the design space. Fig. 4 (osteogenesis) depicts a very large plateau of high performance (>0.93) where $Zn = 1.0\text{--}1.5$ and $Ag = 0.5\text{--}1.0$.

This range is in accordance with the experimental observation that Zn is the major driver behind bone formation during the experimental validations.

Fig. 5 (antibacterial activity) shows a dramatic change in the inhibition zone of the bacteria as a function of increasing Ag concentration, indicating that Ag surpasses other additives to lead the antibacterial activity.

Importantly, in the overlap region, where osteogenesis > 0.93 and antibacterial effect > 14 mm, both conditions only fall in $Zn = 1.0$ and $Ag = 0.5\text{--}1.0$, or similar formulations that match the original experimental work with the $0.5Ag\text{--}1Zn$ and $1Ag\text{--}1Zn$ formulations. This independent computational validation, not only supports the previous experimental work, but formally extends that validation to a continuous design space that offers a clear, suitable recommendation.

**Fig. 4.** Osteogenesis Heatmap.**Fig. 5.** Antibacterial Activity Heatmap.

4. Conclusion

This study involved a data-driven multi-objective optimization framework to rationally design Zn/Ag co-doped bioactive glass nanoparticles (BGNPs) for triple-function bone cancer therapy. Utilizing the extensive experimental dataset of Naruphontjirakul et al. [20] (osteogenic activity, selective anticancer efficacy against MG-63 cells, antibacterial efficacy against both Gram-positive and Gram-negative strains, and biocompatibility with healthy osteoblasts (hFOB 1.19)), we implemented the NSGA-II evolutionary algorithm to find Pareto-optimal Ag/Zn compositions that jointly maximize therapeutic efficacy and performance in each of these three functions. This work suggests that Zn concentrations of greater than 1.0 are required for good mechanical and biological performance of bioactive glass nanosuspensions, while Ag concentrations between 0.01 and 1.0, the levels used in the in-vivo experiment, allowed for good biocompatibility properties while maintaining some antimicrobial properties. Our predictive simulation framework also suggests entire continuum of near-optimal formulations could be substituted and adapted based on the primary therapeutic need (e.g., infection control vs. bone regeneration) at the clinical application stage in the future. Overall, the findings of this work suggest that descriptive biomaterials design could be completed without the need for additional experimentation when high quality experimental data and synthetic methods are available to be used in the framework approach. The framework we developed is a step towards the transition into predictive engineering from true experimentation and provides avenues to advance the development of multifunctional nanotherapeutics to address complex clinical problems, such as reconstructive surgery due to bone cancer resection. We will be developing this framework further to include other therapeutic metals (e.g. Sr, Cu, Ce), dynamic release kinetics, and in-vivo performance prediction based upon a variety of machine learning models. Eventually, these predictive computational approaches should minimize the number of trial-and-error type experiments and thus the time it takes to develop them, working towards personalized biomaterial formulations to individualize the needs of patients.

Author contributions

Michael Askari: Investigation, Writing – original draft, Writing – review & editing; **Lili Arabuli:** Conceptualization, Writing – original draft, Writing – review & editing.

Funding

No funding was received for this study.

Conflict of interest

The authors declare no conflict of interest.

Data availability

No data is available.

REFERENCES

- [1] L. Keil, Bone Tumors: Primary Bone Cancers, *FP essentials* 493 (2020) 22-26.
- [2] R.W. Johnson, L.J. Suva, Hallmarks of bone metastasis, *Calcified tissue international* 102(2) (2018) 141-151.
- [3] A.E. Bădilă, D.M. Rădulescu, A.-G. Niculescu, A.M. Grumezescu, M. Rădulescu, A.R. Rădulescu, Recent advances in the treatment of bone metastases and primary bone tumors: An up-to-date review, *Cancers* 13(16) (2021) 4229.
- [4] M. Vallet-Regi, D. Lozano, B. González, I. Izquierdo-Barba, Biomaterials against bone infection, *Advanced healthcare materials* 9(13) (2020) 2000310.
- [5] Y. Hui, X. Yi, F. Hou, D. Wibowo, F. Zhang, D. Zhao, H. Gao, C.-X. Zhao, Role of nanoparticle mechanical properties in cancer drug delivery, *ACS nano* 13(7) (2019) 7410-7424.
- [6] F. Sharifjafari, D. Nejadkorki, S. Bahadori, Biomedical applications of silica nanoparticle compounds, *Journal of Composites and Compounds* 6(20) (2024).
- [7] Y. Lu, J. Zhang, Y. Chen, Y. Kang, Z. Liao, Y. He, C. Zhang, Novel immunotherapies for osteosarcoma, *Frontiers in Oncology* 12 (2022) 830546.
- [8] S.K. Kapoor, R. Thiyam, Management of infection following reconstruction in bone tumors, *Journal of clinical orthopaedics and trauma* 6(4) (2015) 244-251.
- [9] H. Wei, J. Cui, K. Lin, J. Xie, X. Wang, Recent advances in smart stimuli-responsive biomaterials for bone therapeutics and regeneration, *Bone research* 10(1) (2022) 17.
- [10] M. Yamaguchi, Role of nutritional zinc in the prevention of osteoporosis, *Molecular and cellular biochemistry* 338(1) (2010) 241-254.
- [11] P. Thanasrisuebwong, J.R. Jones, S. Eiamboonserit, N. Ruangsawasdi, B. Jirajirayavej, P. Naruphontjirakul, Zinc-containing sol-gel glass nanoparticles to deliver therapeutic ions, *Nanomaterials* 12(10) (2022) 1691.
- [12] K. Schuhladen, L. Stich, J. Schmidt, A. Steinkasserer, A.R. Boccaccini, E. Zinser, Cu, Zn doped borate bioactive glasses: antibacterial efficacy and dose-dependent in vitro modulation of murine dendritic cells, *Biomaterials science* 8(8) (2020) 2143-2155.
- [13] C. Heras, J. Jiménez-Holguín, A. Doadrio, M. Vallet-Regi, S. Sánchez-Salcedo, A. Salinas, Multifunctional antibiotic-and zinc-containing mesoporous bioactive glass scaffolds to fight bone infection, *Acta biomaterialia* 114 (2020) 395-406.
- [14] S. Chen, S. Greasley, Z. Ong, P. Naruphontjirakul, S. Page, J. Hanna, A. Redpath, O. Tsigkou, S. Rankin, M. Ryan, Biodegradable zinc-containing mesoporous silica nanoparticles for cancer therapy, *Materials Today Advances* 6 (2020) 100066.
- [15] A.M. El-Kady, A.F. Ali, R.A. Rizk, M.M. Ahmed, Synthesis, characterization and microbiological response of silver doped bioactive glass nanoparticles, *Ceramics International* 38(1) (2012) 177-188.
- [16] A. Balamurugan, G. Balossier, D. Laurent-Maquin, S. Pina, A. Rebelo, J. Faure, J. Ferreira, An in vitro biological and anti-bacterial study on a sol-gel derived silver-incorporated bioglass system, *dental materials* 24(10) (2008) 1343-1351.
- [17] J.S. Fernandes, P. Gentile, R.A. Pires, R.L. Reis, P.V. Hatton, Multifunctional bioactive glass and glass-ceramic biomaterials with antibacterial properties for repair and regeneration of bone tissue, *Acta biomaterialia* 59 (2017) 2-11.
- [18] A.A. El-Rashidy, G. Waly, A. Gad, A.A. Hashem, P. Balasubramanian, S. Kaya, A.R. Boccaccini, I. Sami, Preparation and in vitro characterization of silver-doped bioactive glass nanoparticles fabricated using a sol-gel process and modified Stöber method, *Journal of Non-Crystalline Solids* 483 (2018) 26-36.
- [19] V.P.S. Sidhu, R. Borges, M. Yusuf, S. Mahmoudi, S.F. Ghorbani, M. Hosseinkia, P. Salahshour, F. Sadeghi, M. Arefian, A comprehensive review of bioactive glass: synthesis, ion substitution, application, challenges, and future perspectives, *Journal of Composites and Compounds* 3(9) (2021) 247-261.
- [20] P. Naruphontjirakul, P. Kanchanadumkerng, P. Ruenraroengsak, Multifunctional Zn and Ag co-doped bioactive glass nanoparticles for bone therapeutic and regeneration, *Scientific Reports* 13(1) (2023) 6775.
- [21] S. Kargozar, M. Montazerian, E. Fiume, F. Baino, Multiple and promising applications of strontium (Sr)-containing bioactive glasses in bone tissue engineering, *Frontiers in bioengineering and biotechnology* 7 (2019) 161.